Available online at www.sciencedirect.com
SCIENCE DIRECT®
Journal of Solid State Chemistry 176 (2003) 57–61
JOURNAL OF SOLID STATE CHEMISTRY
http://elsevier.com/locate/jssc

Fractal behavior of nanocrystalline ceria–yttria solid solution

P.U. Sastry,[a,*] D. Sen,[a] S. Mazumder,[a] S.V. Chavan,[b] and A.K. Tyagi[b]

[a] *Solid State Physics Division, Bhabha Atomic Research Centre, Mumbai 400085, India*
[b] *Applied Chemistry Division, Bhabha Atomic Research Centre, Mumbai 400085, India*

Received 4 February 2003; received in revised form 3 June 2003; accepted 6 June 2003

Abstract

The fractal characteristics of nano-sized powders of CeO_2–$YO_{1.5}$ solid solutions, prepared by combustion synthesis and calcined at various temperatures, have been investigated by small angle X-ray scattering technique. Results show a mass-fractal behavior for the powders with mass-fractal dimension D_m in the range 2.2–2.6. The estimated particle radii are in the range of 4–15 nm, which is in close agreement with TEM results. For the powders calcined at higher temperatures, the particle interface has a tendency to become rough with a significant growth in the particle size and polydispersity.

1. Introduction

Doped ceria is an important material in view of its potential applications as a solid electrolyte for its use in oxygen concentration cells and in solid oxide fuel cells [1]. It is also used in controlling the air-to-fuel ratio in automobile exhaust [2]. As ceria can be used as a surrogate material for plutonia, its substituted derivatives are also used to simulate thermo-physical properties of plutonia based system [3–5]. Several divalent alkaline-earth and trivalent rare-earth oxides form extensive solid solutions with ceria resulting in significant improvement of properties [6–8]. For example, an aliovalent substitution of trivalent yttria into the lattice of ceria results in the formation of oxygen ion vacancies thereby enhancing the ionic conduction [9,10].

Most of these properties of micro-crystalline materials are modified significantly upon reducing the size of the crystallites to nano-meter scale [11,12]. The properties of such nano-sized powders are influenced by shape, size and size distribution of the constituting particles [13,14], which in turn depend on the characteristics of synthesis. Among the available solution chemistry routes, the combustion technique is capable of producing nano-crystalline powders of the oxide ceramics at lower calcination temperatures in shorter times [15–17]. Generally, powders obtained by this technique possess highest degree of phase purity with improved characteristics like narrow particle size distribution, higher surface area and better sinterability. Because of their relatively high specific surface area and being in a metastable state, these particles often form aggregates which are viewed as fractals. The term 'fractal' originates from the fact that some objects posses a self-similarity (scaling is isotropic) or self-affinity (direction dependent scaling) over a wide range of length scale. The fractal features of powders constituting nano-pores and nano-particles can be probed by small angle X-ray scattering (SAXS) technique [18–20]. For the aggregates in nano-sized powders obtained by combustion synthesis, the mass-fractal nature has been demonstrated [21] experimentally for the first time to best of our knowledge in yittria-based system. Since then, not many studies have focused on this aspect. In this work, the fractal behavior of the nano-sized $Ce_{0.55}Y_{0.45}O_{1.755}$ powders, chosen from the series of CeO_2–$YO_{1.5}$ synthesized by combustion method, has been investigated by SAXS technique. The influence of calcination temperature on the structural features of the powder is discussed.

2. Experimental

2.1. Sample preparation

AR grade cerium nitrate [$Ce(NO_3)_3 \cdot 6H_2O$], yttrium nitrate [$Y(NO_3)_3 \cdot 6H_2O$] were used as oxidants whereas the citric acid ($C_6H_8O_7 \cdot H_2O$) was used as a fuel. They

*Corresponding author. Fax: +91-22-550-5151.
E-mail address: psastry@apsara.barc.ernet.in (P.U. Sastry).

0022-4596/$ - see front matter © 2003 Elsevier Inc. All rights reserved.
doi:10.1016/S0022-4596(03)00344-X

were mixed in the required molar ratios in a minimum volume of de-ionized water to obtain transparent aqueous solutions. This solution, after thermal dehydration (at $\approx 80^{\circ}C$ on a hot plate to remove the excess solvent), resulted in the highly viscous liquid. As soon as the viscous liquid was formed, the temperature of the hot plate was increased to $\approx 250^{\circ}C$. At this stage, the viscous liquid swelled and auto-ignited, with the rapid evolution of large volume of gases to produce voluminous powders. Since the time for which the auto-ignition exists is rather small (<10 s), to remove traces of undecomposed citric acid, nitrates and their decomposition products, the powders obtained after auto-ignition were calcined at 500°C for 1 h to obtain pure, well crystalline ceria powders.

In order to find the influence of temperature on grain growth and fractal behavior, the powders were calcined at six different temperatures viz. 500°C, 600°C, 700°C, 800°C, 900°C, and 1000°C for about an hour in static air and were cooled to room temperature. These samples (labeled S1–S6) were used for SAXS experiments.

2.2. Small angle X-ray scattering (SAXS)

SAXS measurements were carried out using a Rigaku small angle goniometer mounted on a 12 kW rotating anode X-ray generator (Cu$K\alpha$). The intensities were measured by transmission method using a scintillation counter with pulse height analyzer. Scattered X-ray intensity $I(q)$ was recorded as a function of the scattering vector q $(=4\pi\cdot\sin(\theta)/\lambda)$, 2θ being the scattering angle and λ, the wavelength of incident X-rays. The intensities were corrected for sample absorption and smearing effects of collimating slits [22].

3. Method of analysis

SAXS profile of a fractal system follows a power-law over a range of at least one order of magnitude in q. Thus, the scattered intensity $I(q)$ can be described as

$$I(q) \sim q^{-\alpha}, \tag{1}$$

where α is a noninteger related to the fractal dimension. For mass fractals with dimension D_m, $\alpha = D_m \leqslant 3$ whereas for surface fractals with dimension D_s, $\alpha = (6 - D_s) > 3.0$ and $2 \leqslant D_s \leqslant 3$ [18]. Thus, the slope of the scattering curve on log–log scale indicates the type of the fractal. Usually, the power-law scattering (Eq. (1)) is observed in a limited q-range determined by upper and lower cutoff lengths between which the system behaves as a fractal. A detailed discussion on the functionality of $I(q)$ for fractal systems is discussed in literature [18,23,24].

For the analysis of scattering data from a complex system containing multiple levels of structural regimes, an unified formalism was developed [25] recently. Following this formalism, $I(q)$ for a system consisting mass-fractal aggregates of individual particles is given by the equation [25,26]

$$\begin{aligned} I(q) = {} & G_g \exp(-q^2 R_g^2/3) + B_g \exp(-q^2 R_s^2/3) \\ & [\{\mathrm{erf}(qR_g/\sqrt{6})\}^3/q]^m + G_s \exp(-q^2 R_s^2/3) \\ & + B_s[\{\mathrm{erf}(qR_s/\sqrt{6})\}^3/q]^n, \end{aligned} \tag{2}$$

where m is the mass-fractal dimension D_m and n gives the value of $(6 - D_s)$ for the surface-fractal. R_s and R_g are the average radii of gyration of aggregates and basic particles, respectively. Eq. (2) has been used for the analysis of present X-ray data.

In order to obtain the size distribution of the particles, the observed intensity profile has been fitted to that expected for a polydisperse medium of spherical particles [27,28]. The observed intensity can be approximated as

$$I(q) \cong C\left(\int P^2(q,R)D(R)R^6\,\mathrm{d}R\right) S(q), \tag{3}$$

where $P(q,R)$ is the form factor of a spherical scatterer with radius R and is given by

$$P(q,R) = 3[\sin(qR) - qR\cos(qR)]/(qR)^3, \tag{4}$$

C is a constant that depends on the scattering density contrast and $S(q)$ is the inter-particle structure factor. $D(R)$ is the pore size distribution with $D(R)\,\mathrm{d}R$ representing the probability of the pores having a radius between R and $R + \mathrm{d}R$. For a Weibull-type distribution, which is used presently, the function is given by

$$D(R) = [R/a]^{(b-1)} \exp[-(R/a)^b]. \tag{5}$$

For the system of fractal aggregates at larger length scale, $S(q)$ can be expressed as [29]

$$\begin{aligned} S(q) = {} & 1 + [d\Gamma(d-1)/\{(qr_0)^d[1 + 1/(q^2\xi^2)]^{(d-1)/2}\}] \\ & \times \sin[(d-1)\tan^{-1}(q\xi)], \end{aligned} \tag{6}$$

where ξ and $2r_0$ are the upper and lower cutoffs of the fractal whereas d is the fractal dimension D_m.

4. Results and discussion

The fractal features of larger aggregates are reflected in the relatively smaller q-region of the SAXS profiles where as the information about the constituent basic particles is contained in the relatively higher q-region. Fig. 1 shows the (resolution corrected) observed and fitted (to Eq. (2)) intensity profiles of the samples S1–S6 as plotted on log-log scale. In the figure, two distinct fractal dimensions one at low-q region (corresponding to aggregates) and the other at high-q region (corresponding to surface of the basic particles) can be noticed. From the fitted parameters, the power-law exponents

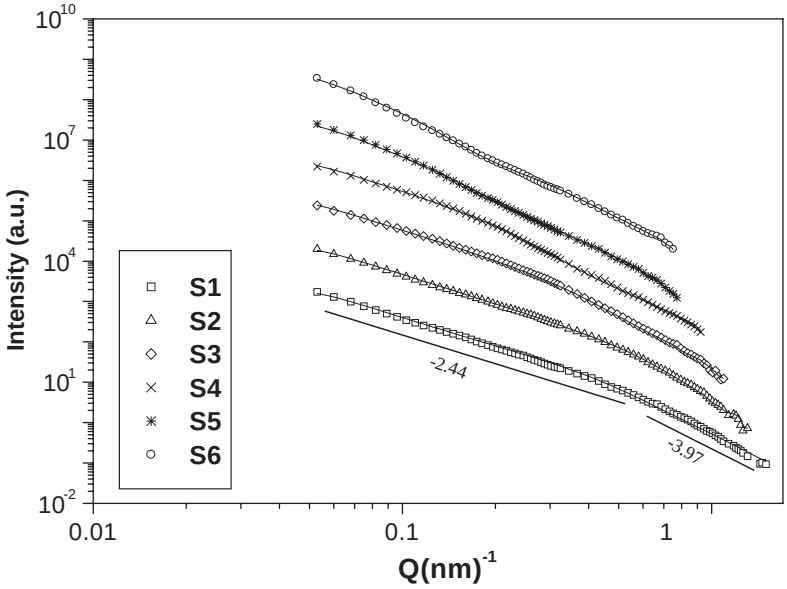

Fig. 1. Log (I) vs. Log (Q) plots of $Ce_{0.55}Y_{0.45}O_{1.755}$ powders prepared by combustion synthesis and calcined at various temperatures in the range 500–1000°C. Typical values of the slopes are indicated for the sample S1.

Table 1
Structural parameters of the powder calcined at various temperatures

Temperature (°C)	Radii of gyration (nm)		Power-law exponents	
	R_g	R_s	$m(=D_m)$	$n(=6-D_s)$
500	75	4.5	2.44	3.97
600	75	5	2.39	4.1
700	85	6.1	2.3	4.0
800	85	8	2.25	3.65
900	80	12	2.57	3.85
1000	85	15	2.55	3.85

and size of the entities are obtained. The values of the power-law exponents (slopes of the lines) at low-q and high-q regions, representing the fractal dimensions, are listed in Table 1. Typical values are also indicated for S1 in Fig. 1. The values of the slopes $(m) \leqslant 3.0$ at lower-q region indicates the mass-fractal nature of the aggregates. A marginal variation of m from one sample to other suggests that the fractal nature of the mass-fractal aggregates remains almost unchanged with calcination temperature. At high-q regions, the value of the exponent (n) varies between 3 and 4 featuring a rough surface for the particles in general (the exponent is 4.0 for smooth surface of the particles). However, the average value of n varies from about 4.0 for S1–S3 to about 3.75 for S4–S6 suggesting that the smooth particle interface has a tendency to become rough beyond the calcination temperature of 800°C. It is noteworthy that the mass-fractal nature has also been observed for the aggregates in yttria-based combustion synthesized powders [21], although the particle interface was noticed to be some what fuzzy in those systems.

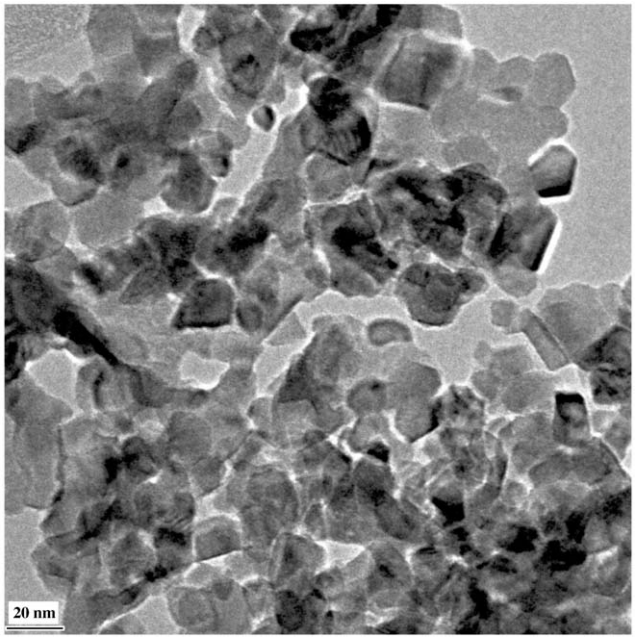

Fig. 2. TEM picture of the sample S2 calcined at 600°C.

The fitted values of the radii of gyration of the aggregates and their constituting particles (assuming a spherical shape for the particles and aggregates) for all the samples are also listed in Table 1. These results show that the average radius R_g of the mass-fractal aggregates varies from 75 to 85 nm whereas the average radius R_s of the basic particles is in the range of 4.5–15 nm for the calcined powders. The order of magnitude of these values are verified by comparing with those obtained by a typical TEM picture (Fig. 2) of S2. As is known, unlike in TEM, SAXS gives the statistically averaged values of

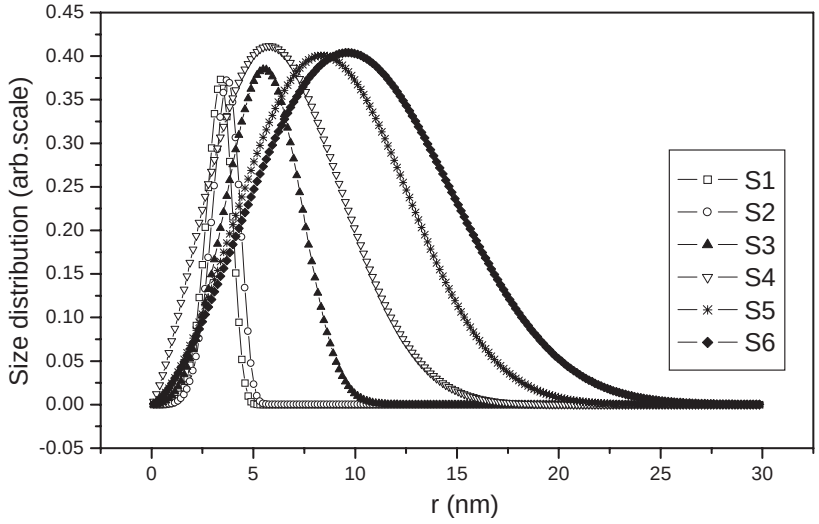

Fig. 3. Particle size distribution in the powders S1–S6 as estimated from SAXS data.

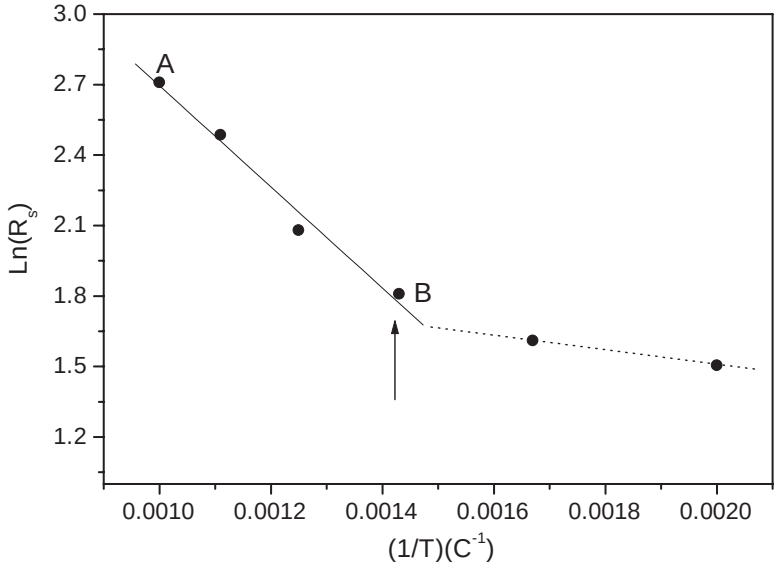

Fig. 4. Variation of Ln (average particle radius) with inverse of the calcination temperature of the powder samples.

the size of the entities. Thus, it can be noticed that the order of magnitude of the sizes obtained by SAXS are fairly consistent with the average values of the sizes of both aggregates and smaller particles from the TEM picture (Fig. 2).

Also, since the TEM picture indicates considerable polydispersity in the size of the particles, we have estimated the particle size distribution $D(R)$ in the powders S1–S6 from SAXS data using Eqs. (3)–(5). As sown in Fig. 3, the narrow size distribution for the particles calcined at lower temperatures becomes significantly wider at higher temperatures. This result, combining with an increase in the radius of the particles with calcination temperatures (Table 1) suggests some sort of rearrangement or mobility of the particles followed by clustering with increase in the temperature. Assuming an Arhenius type dependence ($R_s \propto \exp(-A/T)$) between the average particle size (R_s) and calcination temperature (T) [31,32], interestingly, a plot of $\ln(R_s)$ vs. $(1/T)$ (Fig. 4) shows a linear dependence in the region AB (form about 700°C to 1000°C). This result as well as the significant increase in the polydispersity (wider size distribution) of the particle sizes from 700°C (Fig. 3) suggests that the cluster formation of the particles gains momentum from a calcination temperature between 700°C and 800°C. This in turn is supported by the observed narrowing of (111) diffraction peak (which corresponds to an increase of the average size of the crystallites from 6 nm at lower temperatures to about 14 nm) of the powder calcined at about 800°C [30]. Thus, although the particle aggregation is commonly noticed in the powders obtained by

combustion synthesis [21], the present study suggests that the clustering process is significantly influenced by the calcination temperature of the powders.

The mass-fractal nature of the aggregates formed in the nano-sized powders obtained by combustion synthesis has been modeled theoretically by Tandon and Rosner [26]. Latter, it has been noticed [21] experimentally for the first time in yittria-based nano-sized powders. However, the experimental value (in the range 1.7–1.8) of the mass-fractal dimension D_m was reported to be significantly lower than the theoretical value (in the range 2–3, see Ref. [21]). To our knowledge, no further experimental study on this aspect is done prior to the present one. The mass-fractal nature for the aggregates observed in yittria-based powders [21] and in Ce-based powders (present study) is in agreement with the theoretical model [26]. Further, the value (in the range 2.2–2.6) of D_m for Ce-based powders obtained in our study is higher than that reported in the yittria-based powders [21]. Thus, unlike those in yittria-based powders, the range of values of D_m observed in Ce-based powders agrees well with that of the theoretical model [26]. However, further studies on more variety of nano-sized powders is required to obtained a clear and complete picture on this important and interesting fractal behavior of nano-sized powders prepared by combustion method.

5. Conclusions

The fractal behavior of nanocrystalline ceria–yttria $Ce_{0.55}Y_{0.45}O_{1.755}$ powders prepared by combustion synthesis and calcined at various temperatures has been investigated by SAXS. The estimated size of the particles and the aggregates are in fair agreement with TEM results. The mass-fractal nature including the fractal dimension D_m observed in the present study supports a recently reported theoretical model [21,26]. We have also noticed that the size of the constituent particles increases with calcinations temperature and the clustering of the particles has a tendency to fasten from a calcination temperature between 700°C and 800°C. The variations in size and size-distribution of particles with calcination temperature observed in this study may have significant influence on the optical, catalytic and other related properties of the nanocrystalline doped ceria.

References

[1] Y. Maki, M. Matsuda, T. Kudo, US Patent 3(607), 1971, p. 424.
[2] E.M. Logothetis, Proceedings of the 12th State of-the-Art Symposium on Ceramics in Service of Men, Washington, DC, 1976.
[3] Y.W. Lee, H.S. Kim, S.H. Kim, C.Y. Young, S.H. Na, G. Ledergerber, P. Heimgarbner, M. Pouchon, M. Burghartz, J. Nucl. Mater. 274 (1999) 7.
[4] C. Ganguly, in: I.J. Hasting (Ed.), Proceedings of the Second International Conference CANDU Fuel, Pembroke, Ont., Canada, 1989, p. 398.
[5] M.D. Mathews, B.R. Ambekar, A.K. Tyagi, J. Nucl. Mater. 288 (2001) 83.
[6] V.N. Strekalvskii, G.V. Burov, V.A. Samarina, S.F. Palgue, Z.S. Volchenova, Tr. Inst. Elektrokhim. Akad. Nauk SSSR, Ural. Fil. 3 (1962) 171.
[7] E.K. Keler, N.A. Godina, A.M. Kalinina, Russ. J. Inorg. Chem. 1 (1956) 127.
[8] D.G.M. Bevan, W.W. Barker, R.L. Martin, Proceedings of the Fourth Conference on Rare Earths Research, Phoenix, Ariz, Gordon and Breach, New York, 1965, p. 441.
[9] F.M.B. Marques, G.P. Wirtz, J. Am. Ceram. Soc. 74 (3) (1991) 598.
[10] J. Vanherle, T. Horita, T. Kawada, N. Sakai, H. Yokokawa, M. Dokiya, Solid State Ionics 1255 (1996) 86.
[11] A. Hartridge, A.K. Bhattachary, J. Nanoparticle Res. 3 (2001) 433.
[12] H. Gleiter, J. Appl. Crystallogr. 24 (1991) 79.
[13] T. Matsumoto, J. Suzuki, M. Ohnuma, Y. Kanemitsu, Y. Masumoto, Phys. Rev. B 63 (2001) 195322.
[14] T.P. Martin, U. Naher, T. Bergmann, A. Gohlich, T. Lange, Chem. Phys. Lett. 196 (1991) 113.
[15] Y. Zhou, M.N. Rahaman, Acta Mater. 45 (1997) 3635.
[16] R.D. Purohit, S. Saha, A.K. Tyagi, J. Nucl. Mater. 288 (2000) 7.
[17] R.D. Purohit, A.K. Tyagi, J. Mater. Chem. 12 (2002) 1218.
[18] P.W. Schmidt, J. Appl. Crystallogr. 24 (1991) 414.
[19] P.U. Sastry, D. Sen, S. Mazumder, K.S. Chandrasekaran, Solid State Commun. 114 (2000) 329.
[20] P. Deb, T. Biswas, D. Sen, A. Basumallik, S. Mazumder, J. Nanoparticle Res. 4 (2002) 91.
[21] G. Fagherazzi, S. Ploizzi, M. Bettinelli, A. Speghini, J. Mater. Res. 15 (2001) 586.
[22] P.W. Schmidt, R. Height, Acta Crystallogr. 13 (1960) 480.
[23] J.E. Martin, A.J. Hurd, J. Appl. Crystallogr. 20 (1987) 61.
[24] J. Texeira, J. Appl. Crystallogr. 21 (1988) 781.
[25] G. Beaucage, J. Appl. Crystallogr. 28 (1995) 717.
[26] P. Tandon, D.E. Rosner, Chem. Eng. Commun. 131 (1996) 147.
[27] O. Glatter, O. Kratky, Small Angle X-ray Scattering, Acedamic Press, London, 1982.
[28] A. Gunier, G. Fournet, Small Angle X-rays, Wiely, New York, 1955 (B.C. Walker, trans.).
[29] T. Freltoft, J.K. Jems, S.K. Sinha, Phys. Rev. B 33 (1986) 269.
[30] S.V. Chavan, A.K. Tyagi, J. Mat.Res., Communicated.
[31] E.L. Holmes, W.G. Winegard, Acta Metall. 7 (1959) 411.
[32] D. Sen, T. Mahata, A.K. Patra, S. Mazumder, B.P. Sharma, J. Alloys Compds., 2003, accepted for publication.